Functional Materials 16, No.3 (2009)

$Li_2Zn_2(MoO_4)_3$ crystal as a potential detector for ^{100}Mo 2β-decay search

***N.V.Bashmakova*[1], *F.A.Danevich*[2], *V.Ya.Degoda*[1], *I.M.Dmitruk*[1], *V.M.Kudovbenko*[2], *S.Yu.Kutovyi*[1], *V.V.Mikhailin*[3,4], *S.S.Nagorny*[2], *A.S.Nikolaiko*[2], *S.Nisi*[5], *A.A.Pavlyuk*[6], *S.Pirro*[7], *A.E.Savon*[3], *S.F.Solodovnikov*[6], *Z.A.Solodovnikova*[6], *D.A.Spassky*[4], *V.I.Tretyak*[2], *S.M.Vatnik*[8], *E.S.Zolotova*[6]**

[1]T. Shevchenko Kyiv National University, 01601 Kyiv, Ukraine
[2]Institute for Nuclear Research, MSP 03680, Kyiv, Ukraine
[3]Synchrotron Radiation Laboratory, Physics Faculty, Moscow State University, 119992 Moscow, Russia
[4]D. Skobeltsyn Institute of Nuclear Physics, Moscow State University, 119992 Moscow, Russia
[5]Istituto Nazionale di Fisica Nucleare, Laboratori Nazionali del Gran Sasso, 67010 Assergi (AQ), Italy
[6]A. Nikolaev Institute of Inorganic Chemistry, 630090 Novosibirsk, Russia [7]Sezione Istituto Nazionale di Fisica Nucleare di Milano Bicocca, 20126 Milan, Italy
[8]Institute of Laser Physics, 630090 Novosibirsk, Russia

Received March 30, 2009

Properties of $Li_2Zn_2(MoO_4)_3$ crystals grown by the low-thermal-gradient Czochralski technique have been studied. Chemical composition of the material was tested by ICP-MS mass-spectrometry. Optical properties (refraction, transmittance and reflectivity) have been measured. Luminescence characteristics of crystals under ultraviolet, synchrotron, and X-ray excitation has been studied. Properties and the applicability of $Li_2Zn_2(MoO_4)_3$ crystals as scintillation and bolometric detectors have been checked for the first time.

Изучены свойства кристаллов $Li_2Zn_2(MoO_4)_3$, выращенных методом Чохральского с низким температурным градиентом. Химический состав проверен при помощи ICP-MS масс-спектрометрии. Измерены оптические свойства (преломление, прозрачность и отражение). Люминесцентные характеристики кристаллов изучены при возбуждении ультрафиолетовым, синхротронным и рентгеновским излучениями. Впервые проверены возможности использования кристаллов $Li_2Zn_2(MoO_4)_3$ в качестве сцинтилляционных и болометрических детекторов.

A considerable interest in search for neutrinoless double beta ($0\nu2\beta$) decay [1, 2] is related to the recent evidence for neutrino oscillations which strongly suggests that neutrinos have nonzero mass. However, while oscillation experiments are sensitive only to the neutrino mass difference, measurement of $0\nu2\beta$ decay rate may contribute to the determination of the nature of neutrinos (Majorana or Dirac particle), the neutrino mass scale, and check the lepton number conservation law.

^{100}Mo is among the most promising candidates for 2β decay experiments because of

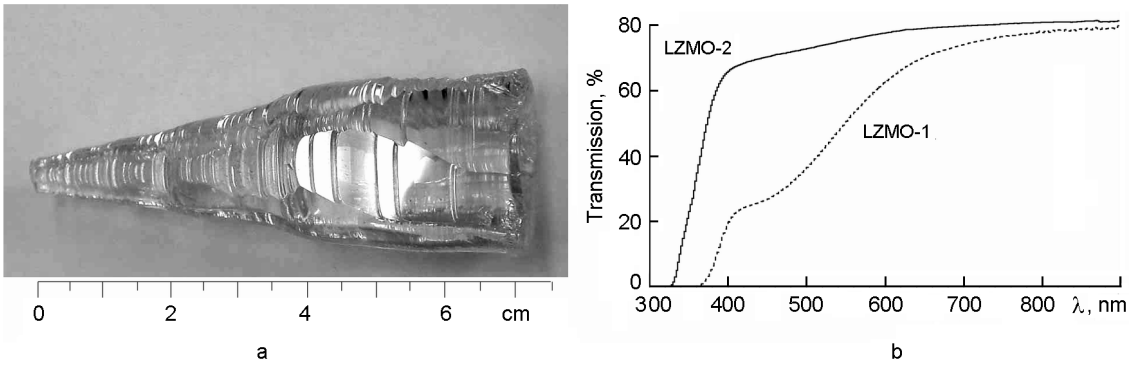

Fig. 1. a) Raw boule of LZMO-2 crystal; b) transmission curves for the LZMO-1 and LZMO-2

its high transition energy ($Q_{2\beta} = 3035$ keV [3]). As a result, the calculated value of the phase space integral for the $0\nu2\beta$ decay of ^{100}Mo is one of the largest among 35 possible 2β decay candidates. Theoretical predictions for the product of half-life by the effective neutrino mass, $T_{1/2}\cdot(m_\nu)^2$, are in the range of $8.0\cdot10^{22}$ to $3.6\cdot10^{27}$ yr·eV^2 [4–7]. From the experimental point of view, the large $Q_{2\beta}$ energy is also preferable to overcome the background problems, since the natural radioactivity background drops sharply above 2615 keV, the energy of γ's from ^{208}Tl decay (^{232}Th family). Contribution from cosmogenic activation, important for the next generation of 2β decay experiments, also decreases at higher energies [8].

A high sensitivity 2β decay experiment demands the following properties of scintillation detectors: high light output, fast response (maximum several hundreds μs), high radiopurity, maximum concentration of isotope studied. Low density and Z value that mean low detection efficiency of background γ quanta are also preferable. If used as bolometric detectors, crystals should have diamagnetic properties to reach low temperature required by this technique. The requirements to radiopurity of crystals for bolometers are even stronger due to rather slow response of these detectors (width of pulses at half of maximum is at the level of 0.1 s). As a result, even low energy processes (as for instance β^- decay of ^{113}Cd in $CdMoO_4$ or $CdWO_4$) may provide difficulties for a bolometric detector operation.

There exist several scintillation crystals containing molybdenum. The most promising of them to search for 2β decay of ^{100}Mo are $CaMoO_4$ [9], $CdMoO_4$ [10], $PbMoO_4$ [11], Li_2MoO_4 [12]. However, all the listed scintillators have some disadvantages: $CaMoO_4$ contains $2\nu2\beta$-active isotope ^{48}Ca in natural Ca with abundance of $\delta = 0.187$ % [13], which creates irremovable background in the energy region of ^{100}Mo 2β decay; $CdMoO_4$ contains β^- active ^{113}Cd ($\delta = 12.22$ %) with the half-life ~$8\cdot10^{15}$ yr; $PbMoO_4$ is contaminated with radioactive ^{210}Pb; Li_2MoO_4 has low light yield.

The purpose of this work was to develop $Li_2Zn_2(MoO_4)_3$ crystals, investigation of their contamination, study of optical and luminescence properties, first test of crystals as scintillation and bolometric detectors. Such a crystal contains 46 % wt. of Mo and probably does not contain radioactive elements, that is of importance for 2β decay experiments with ^{100}Mo. Such crystals could be used also in searches for solar axions (hypothetical particles which could be emitted in deexcitation of $^7Li^*$ in the solar center and resonantly captured by ^7Li nuclei in a detector on the Earth [14]) and different modes of 2β processes in ^{64}Zn, ^{70}Zn, ^{92}Mo, and ^{98}Mo [7, 15,16].

It should be mentioned that the first in the world large optically homogeneous $Li_2Zn_2(MoO_4)_3$ crystals were grown using the specially developed low-thermal-gradient Czochralski technique [17] at the Nikolaev Institute of Inorganic Chemistry (NIIC, Novosibirsk, Russia) in 2006. The first signs of luminescence of these crystals at room temperature were revealed. This hypothesis was checked independently with the samples grown by spontaneous crystallization from stoichiometric solution and also showing a marked response under excitation with α-particles. In this work, two crystals grown at NIIC were studied (labeled hereafter as LZMO-1 and LZMO-2). LZMO-1 was grown from mixture of Li_2CO_3, ZnO, and MoO_3 (3–4 N purity grade) with 5 % excess of Li_2CO_3 and MoO_3 in comparison with the

Table 1. Main properties of $Li_2Zn_2(MoO_4)_3$ crystals

Parameter	Value
Density (g/cm^3)	4.38
Melting point (°C)	890
Crystal system	Orthorhombic
Cleavage plane	Weak (001)
Wavelength of emission maximum (nm)	550–610*
Refractive index at emission maximum	2.0
Effective average decay time** (μs)	0.4

* Depends on the excitation type.
** For α particles at 220 K.

stoichiometric composition. The LZMO-2 boule (Fig. 1a) was grown from additionally purified raw materials, it has nearly conical shape with maximal diameter about 30 mm and total length near 70 mm. The main characteristics of $Li_2Zn_2(MoO_4)_3$ crystals are presented in Table 1. The material is non-hygroscopic and chemically resistant.

To estimate the presence of impurities in the crystals, LZMO-2 was subjected to Inductively Coupled Plasma Mass Spectrometry (ICP-MS, Agilent Technologies model 7500a) at the Gran Sasso National Laboratory, INFN. A sample of the crystal was powdered mechanically inside a clean polyethylene bag to avoid any possible external contamination. Two portions of the sample were etched by the microwave-assisted acid digestion technique (Method EPA 3052) using two different reagents: nitric acid-hydrofluoric acid mixture (4:1) and concentrated hydrofluoric acid. The solutions obtained after centrifugation have been analyzed by ICP-MS.

The concentrations of chemical elements were measured by a semi-quantitative technique. The instrument was calibrated using a single standard solution containing 4 elements to cover the entire mass range. The measured results are presented in Table 2. The errors of the values are at a level of 20–30 %. Moreover, the errors for some elements could be higher because of interference due to production of polyatomic species in the plasma torch including the matrix elements and argon ion. The given results are the averaged values of the measurements for two solutions being in a reasonable agreement. An appreciable contamination of the crystal by Cd and W could be explained by previous using of the growing setup for cadmium tungstate crystals production.

Table 2. Contamination of the $Li_2Zn_2(MoO_4)_3$ crystal measured by ICP-MS analysis

Element	Measured atomic mass	Concentration of element (ppm)	Possible interference
Mg	24	2.6	
Al	27	<0.15	
Sc	45	<0.35	$^{28}Si^{16}O^1H^+$, $^{29}Si^{16}O$
Mn	55	0.9	$^{36}Ar^{19}F^+$, $^{40}Ar^{14}N^1H^+$, $^{39}K^{16}O^+$, $^{38}Ar^{16}O^1H^+$
Fe	57	<1.4	$^{38}Ar^{19}F^+$, $^{40}Ar^{16}O^1H^+$, $^{40}Ca^{16}O^1H^+$
Co	59	<0.14	$^{43}Ca^{16}O^+$, $^{40}Ar^{19}F^+$
Ni	60	0.08	$^{44}Ca^{16}O^+$
Ga	69	0.12	^{68}Zn–^{70}Zn
Ge	72	0.19	$^6Li^{66}Zn^+$
Se	82	0.9	$^{66}Zn^{16}O^+$
Rb	85	<0.01	
Sr	88	0.006	
Ag	107	0.07	
Cd	111	50	$^{95}Mo^{16}O^+$
Sb	121	<0.006	
Cs	133	<0.02	$^{66}Zn^{67}Zn^+$
Ba	137	1.6	
Sm	147	0.3	
W	182	39	
Pt	195	0.6	
Pb	208	0.15	
Bi	209	< 0.001	
Th	232	< 0.001	
U	238	< 0.001	

The refractive index of $Li_2Zn_2(MoO_4)_3$ was measured using a GS-5 goniometer. The sample was shaped as a triangular prism. It was found that the refractive index (n_2) is constant in one polarization plane, while in the other, both lower (n_1^-) and higher (n_1^+) refractive indices were observed for different directions. This indicates that the crystal is biaxial and measurements were performed in two directions which were symmetric to one of the optical axes. Indices are presented for

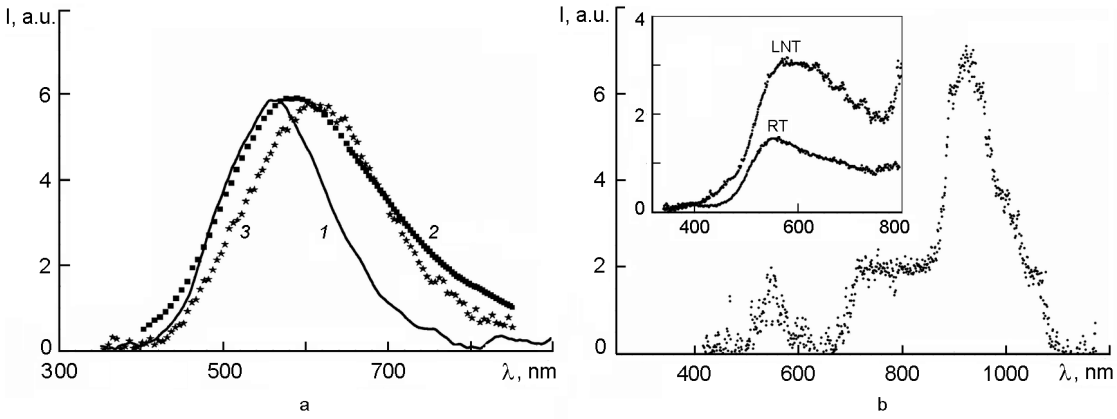

Fig. 2. a) spectrum of $Li_2Zn_2(MoO_4)_3$ luminescence under excitation by ultraviolet (*1*, bold line) and synchrotron radiation at E_{ex} = 4.0 eV and T = 293 K (*2*, squares) and at E_{ex} = 6.0 eV and T = 10 K (*3*, asterisks); b) emission spectrum of $Li_2Zn_2(MoO_4)_3$ crystal under X-ray excitation measured with PMT FEU-83. Inset: emission spectrum in visible region at different temperatures (RT — room; LNT — liquid nitrogen), measured with PMT FEU-106.

Table 3. Refractive indexes of $Li_2Zn_2(MoO_4)_3$ crystal

Wave-length, nm	Refractive indexes		
	n_1^+	n_2	n_1^-
579.0	1.9749(2)	1.9687(2)	1.9622(2)
577.0	1.9746(2)	1.9683(2)	1.9618(2)
546.1	1.9819(2)	1.9757(2)	1.9690(2)
491.6	1.9983(2)	1.9921(2)	1.9850(2)
435.8	2.0237(3)	2.0175(3)	2.0097(3)

five lines of a Hg-lamp (see Table 3). The transmittance of $Li_2Zn_2(MoO_4)_3$ was measured using a Shimadzu UV-3101PC spectrophotometer and is shown in Fig. 1b for about 3 mm thick samples made from LZMO-1 and LZMO-2 crystals. The character of observed curves confirms that additional purification of raw materials decreases light absorption in the crystals. The luminescence spectrum of $Li_2Zn_2(MoO_4)_3$ crystal was studied using a MDR-3 monochromator at room temperature. The photoluminescence was excited by an Ar-laser (the wavelength 351.1 nm). The spectral resolution was 5 nm. The smoothed emission spectrum of a $Li_2Zn_2(MoO_4)_3$ crystal under UV excitation is presented in Fig. 2a (curve *1*, bold line). A wide (FWHM≈160 nm) PL band was observed in visible region with maximum at 562 nm (2.2 eV).

The excitation and reflection spectra in the energy region of 3.7–30 eV were also measured using synchrotron radiation at the SUPERLUMI station (DESY) [18] in the temperature interval of 10–293 K. The measurements were performed on the freshly cleaved vitreous surface. The luminescence spectra were corrected for the setup spectral sensitivity function. The luminescence of $Li_2Zn_2(MoO_4)_3$ at 293 K excited by a 4 eV radiation shows a broad (FWHM≈240 nm) band peaked near 580 nm or 2.01 eV (Fig. 2a, curve *2*, solid squares). The luminescence band measured under excitation with 6 eV energy at T = 10 K was narrowed (FWHM = 210 nm) and its maximum has shifted towards longer wavelengths (λ = 630 nm or 1.97 eV) (Fig. 2a, curve 3, asterisks). The luminescence decay time exceeded 1 μs. The reflection spectrum measured at T = 293 K is presented in Fig. 3a. At least 8 reflection peaks were observed in the wavelength region of 70–300 nm (energies 4–30 eV).

A single luminescence band is generally observed for molybdates of the scheelite structure, as well as for $MgMoO_4$, $ZnMoO_4$ [19–22]. Self-trapped excitons at isolated MoO_4^{2-} complex are ascertained as the luminescence centers for the scheelite type molybdates. However, the crystal structure of $Li_2Zn_2(MoO_4)_3$ differs from the scheelite type, it belongs to the orthorhombic system, space group *Pnma*, with two different types of isolated distorted MoO_4 complexes [23]. Thus, the model of the self-trapped excitons at the isolated MoO_4 complexes can be applied to $Li_2Zn_2(MoO_4)_3$.

The low-energy parts of luminescence excitation spectra measured for emitted light at λ_{em} = 600 nm at T = 10, 170, and 285 K are presented in Fig. 3b. The spectrum edge

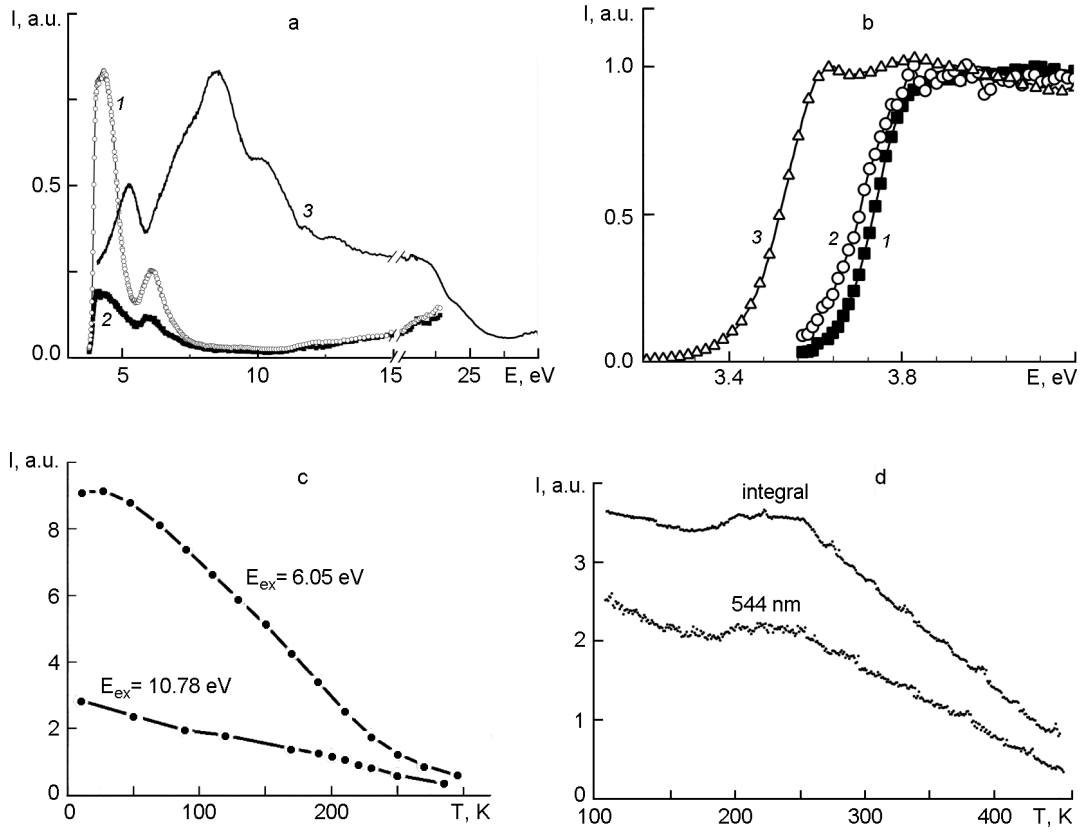

Fig. 3. Temperature dependences of $Li_2Zn_2(MoO_4)_3$ luminescence: a) luminescence excitation spectra measured for λ_{em} = 600 nm at T = 10 K (curve *1*, open circles) and T = 170 K (curve *2*, squares) together with reflectivity of $Li_2Zn_2(MoO_4)_3$ at T = 293 K (*3*, line); b) low-energy part of luminescence excitation spectra measured for λ_{em} = 600 nm at T = 10 K (*1*, solid squares), 170 K (*2*, open circles) and 285 K (*3*, open triangles); c) temperature dependences of $Li_2Zn_2(MoO_4)_3$ luminescence intensity at λ_{em} = 600 nm for excitation energies E_{ex} = 6.1 eV and E_{ex} = 10.8 eV; d) temperature dependences of luminescence intensity under X-ray excitation for the wavelengths near the emission maximum (544 nm) and for integral spectrum.

is seen to be shifted to the low-energy region as the temperature increases. Perhaps it follows from the temperature shift of the fundamental absorption edge. The dip in the luminescence excitation spectrum at 5.5 eV (~220 nm) is due to the increase of the near-surface losses in the region of the first reflection peak (Fig. 3a, curves *1*–*2*). As the excitation energy rises, the intensity drops almost to zero at 8 eV (150 nm). The slow increase in the luminescence excitation intensity at $E > 11$ eV ($\lambda < 115$ nm) is ascribed to the multiplication processes with repeated formation of low-energy electron-hole pairs.

It is to note that the most of reflection peaks at λ = 100–200 nm (6–11 eV, Fig. 3a, curve *3*) does not appear in the excitation spectra due to the low intensity of the latter. Such a behavior can be explained by the existence of efficient energy relaxation centers competitive to the exciton-type luminescence ones. As the excitation energy increases, the mean distance between the separated electron and hole increases, too. Thus, the probability for the separated electron an hole to be bound into and exciton decreases because charge carriers can be intercepted by the competitive relaxation channels during the migration through the crystal. The presence of the competitive relaxation channel affects also the temperature dependence of the luminescence intensity (see Fig. 3c). As there is only a single luminescence band under VUV-excitation, the competitive energy relaxation centers can be concluded to have non-radiative character. The origin of such centers is not clear. Anyway, their presence should decrease the scintillation yield of the crystal.

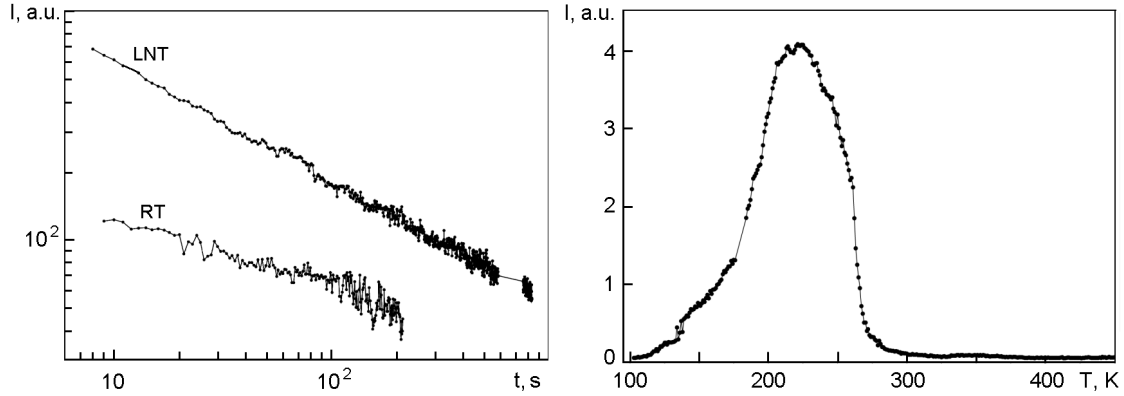

Fig. 4. a) Time dependences of $Li_2Zn_2(MoO_4)_3$ crystal luminescence intensity after X-ray excitation at room (RT) and liquid nitrogen (LNT) temperatures; b) thermoluminescence of $Li_2Zn_2(MoO_4)_3$ crystal after X-ray excitation at liquid nitrogen temperature.

The luminescence spectra of a 5×5×1 mm^3 sample under excitation by integral X-ray spectrum from a BHV7 tube with Rhenium anode (20 kV, 20 mA) measured using a MDR-2 high aperture monochromator and FEU-83 photomultiplier (spectral sensitivity 600–1200 nm) and FEU-106 (300–800 nm) one are shown in Fig. 2b. The X-luminescence spectrum consists of several weak bands in visible region, and of several intense ones in IR range. Spectra in visible range measured at 293 K and 113 K have practically the same shape but differ in intensity.

The temperature dependences of the $Li_2Zn_2(MoO_4)_3$ X-luminescence intensity measured at $\lambda = 600$ nm for the excitation energies $E_{ex} = 6.05$ eV and $E_{ex} = 10.78$ eV are shown in Fig. 3c. The dependences of $Li_2Zn_2(MoO_4)_3$ X-luminescence intensity on temperature (85–450 K) measured in wide interval of wavelengths (integral) and in the narrow region near the emission maximum (544 nm) are presented in Fig. 3d. The intensity slowly falls down, however, remains still noticeable even up to 450 K. A low maximum at 200–250 K can be explained by superposition of thermally stimulated luminescence (see below).

At room temperature, a slow decrease of X-luminescence intensity is seen (Fig. 3d) that can be due to two causes: (i) increasing fraction of radiationless recombination on recharged traps during X-ray radiation and accumulation of light sum at deep traps; and (ii) formation of color centers that absorb the luminescence radiation. The first process is supposed to be dominant, as dose dependence of X-luminescence intensity has exponential character. A minor increase of luminescence intensity at the excitation start at 85 K (when the quantity of deep traps is much more than at room temperature) confirms this assumption.

The total luminescence intensity of $Li_2Zn_2(MoO_4)_3$ is more than three orders of magnitude lower than that of commonly used ZnS(Cu) luminophor. This evidences an intense radiationless recombination of electronic excitations. A temperature quenching of the luminescence is observed, however, it cannot be described by the Mott formula ($I = I_{max}/(1 + Ae^{-E/kT})$ even at the temperatures higher than 250 K. It could be due to contribution from several processes resulting both in internal and external extinguishing of luminescence. Such a behavior is typical of many oxides.

The long-term phosphorescence (Fig. 4a) and thermally stimulated luminescence (TSL, Fig. 4b) under X-ray excitation were measured at room (293 K, RT) and liquid nitrogen (85 K, LNT) temperatures. The results obtained testify presence of traps in $Li_2Zn_2(MoO_4)_3$ crystals. It should be emphasized that the phosphorescence attenuation (Fig. 4a) meets a hyperbolic law that evidences the recombination character of luminescence in the material. The TSL was observed in a wide temperature interval, however, the light is emitted mainly at 200–240 K. This conclusion does not contradict the assumption about existence of autolocalised excitons as luminescence centers. During the phosphorescence, regeneration of autolocalised exciton after release of one of charge carriers from the trap could take place. The possibility of such regeneration was shown, e.g. for BaF_2 [24]. Therefore, thermostimulated regeneration of self-

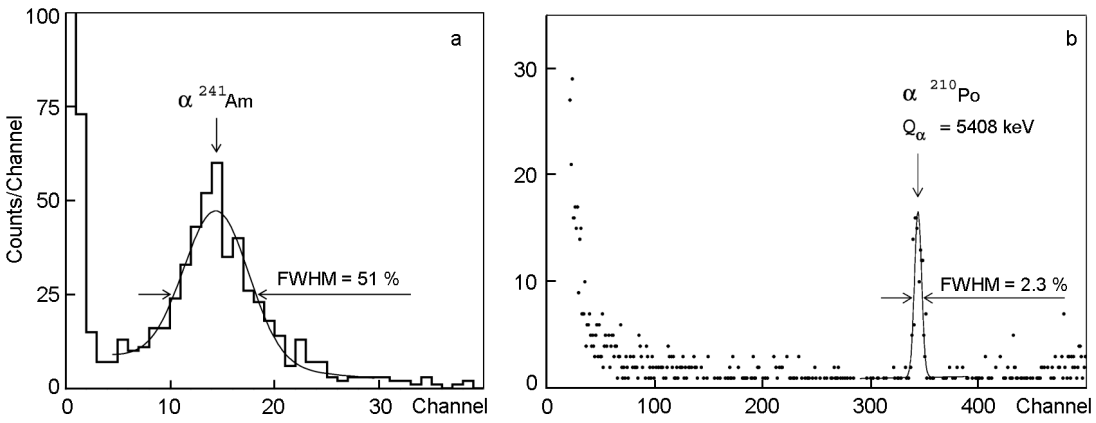

Fig. 5. Spectrometric properties of $Li_2Zn_2(MoO_4)_3$ crystals: a) energy spectrum of ^{241}Am α-particles (E_α = 5.25 MeV) measured using a 5×5×1.3 mm^3 sample as scintillator; b) energy spectrum measured using a 20×10×2 mm^3 crystal at 10 mK as bolometer.

trapped excitons after X-ray excitation may result in a hyperbolic dependence of phosphorescence decay in $Li_2Zn_2(MoO_4)_3$. Attempts are reasonable to enhance the light output of $Li_2Zn_2(MoO_4)_3$ by activation with doping elements which could create more efficient light emission centers.

The spectrometric characteristics were measured in the temperature range of 123–293 K using a 5×5×1.3 mm^3 sample prepared from the LZMO-2 crystal. The crystal was viewed by the Philips XP2412 bialkali PMT through a high purity quartz light guide ∅4.9×25 cm. The $Li_2Zn_2(MoO_4)_3$ sample and the light guide were wrapped with the PTFE tape as reflector. A Dow Corning Q2-3067 optical couplant was used to provide optical contact of the scintillator with the light guide, and of the light guide with the PMT. The crystal and the main part of the light guide were placed into a Dewar vessel, while the PMT was thermally isolated from the vessel. This way, the PMT temperature was kept stable (about RT) during the measurements. The Dewar vessel was periodically filled by small amounts of liquid nitrogen to cool the crystal. Its temperature was measured using a flexible chromel-alumel thermocouple. A 20 MC/s transient digitizer was used to accumulate several hundreds of $Li_2Zn_2(MoO_4)_3$ scintillation pulses at each temperature. Then the recorded pulse shapes were used to provide the energy spectra by calculating the area of each signal from the starting point up to 10 μs.

A collimated ^{241}Am α particle source was used in the measurements. As it was checked by surface-barrier detector, the α particle energy was reduced to about 5.25 MeV due to passing through the collimator (~1 mm of air). Fig. 5a shows the energy spectrum of the α particles measured by the $Li_2Zn_2(MoO_4)_3$ scintillator at 223 K. The energy resolution of 51 % was obtained for α-particles of ^{241}Am source. The relative photoelectron yield of $Li_2Zn_2(MoO_4)_3$ was estimated to be about 3–4 % with respect to 21×13×9 mm^3 $CaMoO_4$ crystal of [9] at 220 K. In measurements [9], taking into account a much longer decay time of $CaMoO_4$ scintillator (≈100 μs), the energy spectrum of $CaMoO_4$ was plotted by calculating the area of each signal from the starting point up to 380 μs. The temperature dependence of the $Li_2Zn_2(MoO_4)_3$ light output measured with α particles in temperature range 123–293 K agrees with the behavior observed under X-ray irradiation.

It should be noted that most of inorganic crystal scintillators can also be applied as scintillating low-temperature bolometers with simultaneous recording of both light and heat signals [16]. A great advantage of this technique is due to excellent energy resolution (at the level of a few keV in a wide energy interval) and discrimination ability of different ionizing particle types. To check such a possibility, a $Li_2Zn_2(MoO_4)_3$ crystal sample of 20×10×2 mm^3 size was tested at 10 mK as a cryogenic detector in the setup described in [16]. A clear phonon signal was detected. The energy spectrum accumulated with the sample is shown in Fig. 5b. The peak at #344 channel with FWHM = 2.3 % and area 128±15 counts

can be ascribed to internal contamination of the sample with ^{210}Po (Q_a = 5408 keV).

To conclude, the high optical quality $Li_2Zn_2(MoO_4)_3$ crystals have been grown by the low-thermal-gradient Czochralski technique. The material contamination with other chemical elements measured by ICP-MS does not exceed the ppm level except for Mg (2.6 ppm), Cd (50 ppm), and W (39 ppm). The refractive indices of $Li_2Zn_2(MoO_4)_3$ were measured in the 463–579 nm wavelength range. The crystal was found to be biaxial. The values of refractive indexes are in the range 1.96–2.02. The transmittance of $Li_2Zn_2(MoO_4)_3$ was measured for two samples grown from raw materials 3–4 N purity grade, and from additionally purified raw materials. The additional purification of raw materials decreases absorption in crystals thus suggesting that a further purification could significantly improve the crystal optical properties. The luminescence under UV, synchrotron and X-ray excitation was studied. A weak luminescence was observed in visible range with a maximum at 550–610 nm, depending on the excitation kind. The crystals show a considerable luminescence in IR range under X-ray excitation. The temperature dependence of the luminescence intensity was measured in the 10–293 K range under synchrotron irradiation, and under X-ray excitation. The luminescence intensity increases with decreasing temperature. Radiationless transitions dominate in recombination processes, thus causing a rather low light output level of the crystals. Scintillation properties of $Li_2Zn_2(MoO_4)_3$ were tested with α particles from a ^{241}Am source in the 123–293 K temperature range. At 223 K, the photon yield of $Li_2Zn_2(MoO_4)_3$ is ≈4 % relatively to $CaMoO_4$. The temperature dependence of light yield measured with α particles agrees with the behavior obtained under X-ray irradiation.

The applicability of crystals as cryogenic bolometric detectors was demonstrated for the first time. A clear phonon signal was detected at 10 mK and energy resolution FWHM = 2.3 % was obtained for 5408 keV α particles. Despite scintillation properties of $Li_2Zn_2(MoO_4)_3$ crystals are worse than those of other crystals containing Mo, they can be used as bolometric detectors to search for 2β decay of ^{100}Mo. As a next step, we intend to produce $Li_2Zn_2(MoO_4)_3$ crystals from raw materials selected for ultra-low background γ- and α-spectrometry to check further possibilities to use material as cryogenic detectors in search for 2β decay of molybdenum.

Acknowledgements. F.A.Danevich, V.M.Kudovbenko, S.S.Nagorny, A.S.Nikolaiko, V.I.Tretyak were supported in part by the "Kosmomikrofizyka" (Astroparticle Physics) Project at the National Academy of Sciences of Ukraine. The investigations by V.V.Mikhailin, A.E.Savon, D.A.Spassky were supported by Grant DFG 436 RUS 113/437-3. We are grateful to Prof.G.Zimmerer for providing the opportunity to perform measurements at the SUPERLUMI station.

References

1. F.T.Avignone III, S.R.Elliott, J.Engel, *Rev. Mod. Phys.*, **80**, 481 (2008).
2. Yu.G.Zdesenko, *Rev.Mod.Phys.*, **74**, 663 (2002).
3. G.Audi, A.H.Wapstra, C.Thibault, *Nucl.Phys. A*, **729**, 337 (2003).
4. V.A.Rodin, A.Faessler, F.Simkovic et al., *Nucl.Phys.A*, **766**, 107 (2006); **793**, 213 (2007).
5. M.Kortelainen, J.Suhonen, *Phys.Rev.C*, **76**, 024315 (2007).
6. J.Suhonen, M.Kortelainen, *AIP Conf.Proc.*, **972**, 128 (2008).
7. V.I.Tretyak, Yu.G.Zdesenko, *At.Data Nucl. Data Tables*, **80**, 83 (2002).
8. Yu.G.Zdesenko, F.T.Avignone III, V.B.Brudanin et al., *Astropart.Phys.*, **23**, 249 (2005).
9. A.N.Annenkov, O.A.Buzanov, F.A.Danevich et al., *Nucl.Instr.Meth.Phys. Res. A*, **584**, 334 (2008).
10. V.B.Mikhailik, H.Kraus, D.Wahl et al., *Phys. Status Solidi.B*, **242**, R17 (2005).
11. F.A.Danevich, Yu.G.Zdesenko, V.N.Kouts et al., in: Abstr. 6th Int. Workshop on Low Temp. Detectors, Beatenberg/Interlaken, Switzerland, 28 Aug.–1 Sept. 1995, p.59.
12. O.P.Barinova et al., Abstr. of Nat. Conf. on Crystal Growing (NCCG 2006), Moscow, October 23–27, 2006, p.281.
13. J.K.Bohlke, J.R.DeLaeter, DeBievre et al., *J. Phys.Chem.Reference Data*, **34**, 57 (2005).
14. P.Belli, R.Bernabei, R.Cerulli et al., *Nucl. Phys.A*, **806**, 388 (2008).
15. P.Belli, R.Bernabei, F.Cappella et al., *Phys. Lett.B*, **658**, 193 (2008).
16. S.Pirro, C.Arnaboldi, J.W.Beeman et al., *Nucl.Instrum.Meth.Phys. ResA*, **559**, 361 (2006).
17. A.A.Pavlyuk, Ya.V.Vasiliev, L.Yu.Kharchenko et al., in: Proc. Asia Pacific Society for Adv. Mat. APSAM-92, 26–29 April 1992, Shanghai, Published in Japan 1993, p.164.
18. G.Zimmerer, *Radiat.Meas.*, **42**, 859 (2007).
19. I.V.Kitaeva, V.N.Kolobanov, V.V.Mikhailin et al., in: Proc. 8th Int. Conf. on Inorganic Scin-

tillators (SCINT 2005), Alushta, Ukraine, 2005, p.44.
20. D.Spassky, A.Vasil'ev, I.Kamenskikh et al., *Phys. Stat. Solidi A*, **1–5**, 206,1579 (2009)
21. Spassky, S.Ivanov, I.Kitaeva et al., *Phys. Stat. Solidi (c)*, **2**, 65 (2005).
22. V.B.Mikhailik, H.Kraus, D.Wahl et al., *Nucl. Instr. Meth.Phys.Res. A*, **562**, 513 (2006).
23. Xue Li-Ping, Lin Zhang, Huang Feng et al., *Chinese J. Struct. Chem.*, **26**, 1208 (2007).
24. Kazuie Kimura, Wan Hong, *Phys. Rev. B*, **58**, 6081 (1998).

Кристал $Li_2Zn_2(MoO_4)_3$ як можливий детектор 2β-розпаду ^{100}Mo

Н.В.Башмакова, Ф.А.Даневич, В.Я.Дегода, І.Н.Дмитрук, С.Ю.Кутовой, В.В.Михайленко, С.С.Нагорний, С.Нісі, А.С.Ніколайко, А.А.Павлюк, С.Пірро, А.Е.Савон, Д.А.Спасський, С.Ф.Солодовников, З.А.Солодовникова, В.І.Третяк, С.М.Ватник, Е.С.Золотова

Досліджено властивості кристалів $Li_2Zn_2(MoO_4)_3$, вирощених методом Чохральського з низьким температурним градієнтом. Хімічний склад зразків перевірено за допомогою ICP-MS мас-спектрометрії. Виміряно оптичні характеристики (заломлення, прозорість та відбивання). Люмінесцентні характеристики кристалів досліджено при збудженні ультрафіолетовим, синхротронним та рентгенівським випромінюваннями. Вперше перевірено можливості використання кристалів $Li_2Zn_2(MoO_4)_3$ як сцинтиляційних та болометричних детекторів.